International Journal of Bifurcation and Chaos, Vol. 24, No. 8 (2014) 1440012 (10 pages)

DOI: 10.1142/S0218127414400124

Bifurcations of Chaotic Attractors in One-Dimensional Piecewise Smooth Maps

Viktor Avrutin
DESP, University of Urbino, Italy
and IST, University of Stuttgart, Germany
Avrutin.Viktor@ist.uni-stuttgart.de

Laura Gardini
DESP, University of Urbino, Italy
Laura.Gardini@uniurb.it

Michael Schanz
IPVS, University of Stuttgart, Germany
Michael.Schanz@ipvs.uni-stuttgart.de

Iryna Sushko
Institute of Mathematics,
National Academy of Sciences of Ukraine, Ukraine
Sushko@imath.kiev.ua

Received February 2, 2014

In this work, we classify the bifurcations of chaotic attractors in 1D piecewise smooth maps from the point of view of underlying homoclinic bifurcations of repelling cycles which are located before the bifurcation at the boundary of the immediate basin of the chaotic attractor.

Keywords: One-dimensional maps; piecewise smooth maps; discontinuous maps; multiband chaotic attractors; homoclinic bifurcations; crises.

1. Introduction

It is well known that dynamical systems defined by piecewise smooth functions exhibit several phenomena which cannot occur in smooth systems, such as for example, border collision bifurcations, sliding, chattering, etc. [di Bernardo *et al.*, 2008]. One such phenomenon is the persistence of chaotic attractors under parameter perturbations, referred to as *robust chaos* [Banerjee *et al.*, 1998]. In this case, there is an open region in the parameter space, called chaotic domain or domain of robust chaos, corresponding to chaotic attractors only. It is well-known that these attractors may undergo bifurcations (frequently referred to as *crises*) leading to a sudden change of the shape of the attractor, or to a change of the number of its bands (connected components). Such bifurcations may be organized in complex bifurcation scenarios [Avrutin & Schanz, 2008; Avrutin & Sushko, 2012]. At the boundary of a chaotic domain similar bifurcations may lead to a transformation of a chaotic attractor into a chaotic repeller. Although such bifurcations were intensively studied by many authors, there is not a unique widely accepted terminology in this field. In particular, *interior crises* [Grebogi *et al.*, 1982, 1983, 1987; Ott, 1993] can be seen as a special class of *contact bifurcations* [Mira & Narayaninsamy, 1993; Gardini *et al.*, 1996; Mira *et al.*, 1996a; Mira *et al.*, 1996b; Fournier-Prunaret *et al.*, 1997; Maistrenko *et al.*, 1998] called also *explosions of*

recurrent points in [Robert *et al.*, 2000; Alligood *et al.*, 2002]. Also the notions of *boundary crises*, *exterior crises* and *final bifurcations* refer to similar phenomena.

It is known that the bifurcations mentioned above are related to particular *homoclinic bifurcations* of repelling cycles located at the *boundary of the immediate basin* of the attractor [Mira *et al.*, 1996a]. The aim of the present paper is to clarify which kinds of homoclinic bifurcations are responsible for which type of bifurcations of chaotic attractors, restricting ourselves in this work to 1D maps.

The homoclinic bifurcations of repelling cycles mentioned above are related to the appearance of *critical homoclinic orbits* to these cycles, that means homoclinic orbits including critical points. Following [Mira *et al.*, 1996a], a critical point of a continuous (smooth or piecewise smooth) function f is defined as the value of f at its local extremum (smooth or nonsmooth).[1] If f is a discontinuous function, then its limiting values at discontinuity points are called critical points as well [Gardini *et al.*, 2011]. A homoclinic orbit is persistent under parameter perturbation iff it is noncritical. A critical homoclinic orbit which includes a point of a smooth local extremum (fold point) is called degenerate. It is proved in [Marotto, 1978; Gardini, 1994; Marotto, 2005] that the existence of a nondegenerate homoclinic orbit $\mathcal{O}$ to a repelling fixed point x^* of a smooth map f in $\mathbb{R}^n$ implies the existence of an invariant set Λ in a neighborhood of $\mathcal{O}$, on which f is chaotic. Note that the same result applies also for a nondegenerate heteroclinic connection between two repelling fixed points x^* and x^{**}, which is defined as a union of two heteroclinic orbits, one from x^* to x^{**}, and the other one from x^{**} to x^*.

In [Gardini *et al.*, 2011] this result is extended to piecewise smooth (continuous and discontinuous) maps. It is proved that the existence of a noncritical homoclinic orbit implies the existence of chaos in a neighborhood of the orbit and that the appearance of infinitely many homoclinic orbits, also called an Ω-explosion, is associated with the existence of a critical homoclinic orbit. First of all, this result provides a powerful tool for the proof of existence of chaos. Moreover, it suggests also a way how to formulate the condition of the bifurcations of chaotic attractors mentioned above. Indeed, the existence of a critical homoclinic orbit implies that *a critical point is preperiodic* to the repelling cycle undergoing a homoclinic bifurcation, i.e. it is mapped on a point of the cycle within a finite number of iteration steps.

Additionally, for the description of bifurcations of chaotic attractors in a 1D map f the following facts are essential:

(1) Boundaries of a chaotic attractor are given by critical points of the map and their images.
(2) A multiband chaotic attractor in a continuous map is always cyclic, while in a discontinuous map it may be acyclic (see [Avrutin *et al.*, 2014]). Therefore, investigation of an m-band chaotic attractor of a continuous map f can be reduced to the investigation of a one-band attractor of the iterated map f^m. When dealing with a discontinuous map, this is not always possible.
(3) Chaotic attractors in piecewise linear maps include necessarily at least one border point. Therefore, in piecewise linear maps with one border point the immediate basin boundaries of any chaotic attractor cannot include the border point and are formed by one or several cycles and possibly also by their preimages. Similar result applies also to piecewise smooth maps without smooth extrema.

Below, we illustrate the bifurcations of chaotic attractors using the most simple example, namely the family of piecewise linear maps $f : \mathcal{I} \to \mathcal{I}$, $\mathcal{I} \subset \mathbb{R}$, defined by

$$x_{n+1} = f(x_n) = \begin{cases} f_{\mathcal{L}}(x_n) = a_{\mathcal{L}} x_n + \mu_{\mathcal{L}} & \text{if } x_n < 0 \\ f_{\mathcal{R}}(x_n) = a_{\mathcal{R}} x_n + \mu_{\mathcal{R}} & \text{if } x_n > 0 \end{cases} \quad (1)$$

where $a_{\mathcal{L}}$, $a_{\mathcal{R}}$, $\mu_{\mathcal{L}}$, $\mu_{\mathcal{R}}$ are real parameters. In general, i.e. for $\mu_{\mathcal{L}} \neq \mu_{\mathcal{R}}$, map (1) is discontinuous. Note that in this case we do not define the value $f(0)$, as it is not relevant for the bifurcation structure of the parameter space. By contrast, the values $f_{\mathcal{L}}(0)$ and $f_{\mathcal{R}}(0)$ are well-defined and represent critical points of f. In the particular case $\mu_{\mathcal{L}} = \mu_{\mathcal{R}} = \mu$, map (1) is continuous and represents the well-known

[1]This notion, going back to the works by Julia and Fatou, differs from the definition commonly used in analysis where a point of a local extremum is called critical, and not the value at this point.

skew tent map

$$x_{n+1} = f(x_n) = \begin{cases} f_{\mathcal{L}}(x_n) = a_{\mathcal{L}} x_n + \mu & \text{if } x_n \le 0 \\ f_{\mathcal{R}}(x_n) = a_{\mathcal{R}} x_n + \mu & \text{if } x_n \ge 0 \end{cases}. \quad (2)$$

The main advantage of maps (1) and (2) for our purposes is the possibility to calculate analytically the points of the cycles (of any period) undergoing homoclinic bifurcations. Thus, the related bifurcation conditions can be expressed in an explicit form with respect to the parameters.

2. Merging Bifurcation

Consider a 1D piecewise smooth map f depending smoothly on a parameter ν. Assume the existence of a value $\nu = \nu_0$ such that for ν in a one-side neighborhood of ν_0 the map f has a chaotic attractor $\mathcal{A}_k$ consisting of $k \ge 2$ bands,[2] *and there is a repelling n-cycle $\mathcal{O}_n$, $1 \le n < k$, with a* negative *eigenvalue, whose points are located at the* boundary of the immediate basin *of $\mathcal{A}_k$. The* merging bifurcation[3] *occurs if at $\nu = \nu_0$ the attractor $\mathcal{A}_k$ collides with the cycle $\mathcal{O}_n$ and the bands of the attractor contacting the cycle $\mathcal{O}_n$, merge pairwise.*

As the boundaries of a chaotic attractor are formed by critical points and their images, at the bifurcation moment the cycle $\mathcal{O}_n$ collides with some of them (in other words, the corresponding critical point becomes preperiodic to $\mathcal{O}_n$). This leads to the appearance of a homoclinic orbit to $\mathcal{O}_n$, which is critical at the bifurcation value. Accordingly, the cycle undergoes a homoclinic bifurcation. Being nonhomoclinic before the bifurcation, the cycle necessarily becomes double-side homoclinic after (as a cycle with a negative eigenvalue cannot be one-side homoclinic).

Clearly, as the bands of $\mathcal{A}_k$ merge pairwise, at the bifurcation moment $2n$ boundaries of the attractor have a contact with its immediate basin. As a result of the merging bifurcation the number of bands of the chaotic attractor is decreased by n. In a particular case, typical for piecewise smooth continuous maps (see Example 2.1 below), a chaotic attractor undergoing a merging bifurcation has $k = 2n$ bands before the bifurcation and collides with a cycle of period n. Then all the bands merge pairwise and their number after the merging bifurcation is halved.

Example 2.1. Figure 1 shows the transition from a six- to a three-band chaotic attractor in the skew tent map (2), occurring for decreasing value of $a_{\mathcal{R}}$ at $\gamma_{\mathcal{RL}^2}$. The repelling cycle[4] involved in the bifurcation is $\mathcal{O}_{\mathcal{RL}^2}$, and its eigenvalue $\lambda = a_{\mathcal{R}} a_{\mathcal{L}}^2$ is negative as $a_{\mathcal{R}} < 0$. Before the bifurcation, the cycle is not homoclinic.

For decreasing value of $a_{\mathcal{R}}$, the bands of the attractor grow and at the bifurcation value they merge pairwise colliding with the points of the cycle $\mathcal{O}_{\mathcal{RL}^2}$. Clearly, after the bifurcation, the cycle becomes double-side homoclinic. As one can see in Fig. 1, to calculate the parameter values related to the merging bifurcation, one has to solve any of the equations $x_0^{\mathcal{RL}^2} = c_6$, $x_1^{\mathcal{RL}^2} = c_7$, and $x_2^{\mathcal{RL}^2} = c_8$, where $c_i = f^i(c)$, and $c = f(0) = \mu$. Clearly, the first equation contains the image of the critical

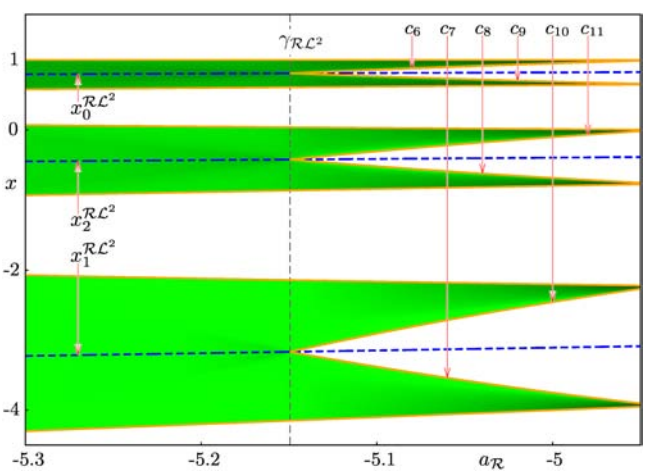

Fig. 1. Merging bifurcation $\gamma_{\mathcal{RL}^2}$ in the skew tent map (2) related to a homoclinic bifurcation of the 3-cycle $\mathcal{O}_{\mathcal{RL}^2}$. Parameters: $a_{\mathcal{L}} = 0.45$, $\mu = 1$.

[2]As the map is 1D, the bands of the attractor as well as the gaps between bands are real intervals.

[3]According to the definition given in [Grebogi *et al.*, 1983], this bifurcation represents a special type of an interior crisis. In some works, this bifurcation is referred to as a *merging crisis* (although this term is more frequently used for *attractor-merging crises* related to collisions of two or more previously coexisting chaotic attractors), or as a *band-merging bifurcation* [Crutchfield & Young, 1990; Kaneko, 1989].

[4]Here and in the following, we use the standard notation for a symbolic sequence associated with a cycle of a map defined on two partitions: a point of a cycle located in the left half-axis $x < 0$ is represented by the letter $\mathcal{L}$ and a point located in the right half-axis $x > 0$ with the letter $\mathcal{R}$.

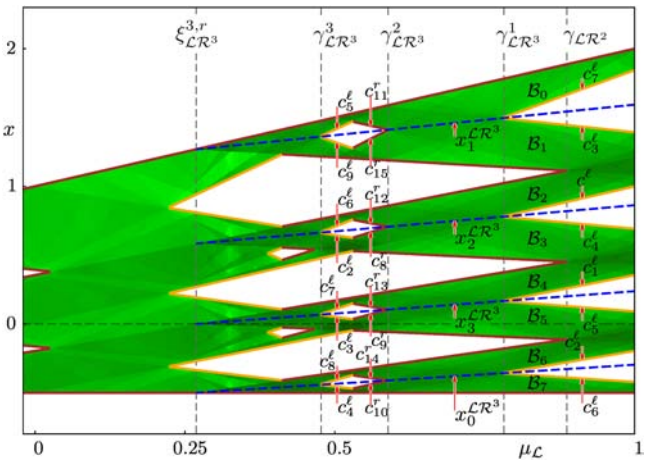

Fig. 2. Merging bifurcations $\gamma^1_{\mathcal{LR}^3}$, $\gamma^2_{\mathcal{LR}^3}$ and $\gamma^3_{\mathcal{LR}^3}$ related to homoclinic bifurcations of the 4-cycle $\mathcal{O}_{\mathcal{LR}^3}$ in map (1). Parameters: $a_{\mathcal{L}} = -2$, $a_{\mathcal{R}} = 0.855$, $\mu_{\mathcal{R}} = -0.5$.

point of the lowest rank and is therefore most easy to solve.

Example 2.2. Figure 2 shows several merging bifurcations occurring in the discontinuous map (1). The 4-cycle $\mathcal{O}_{\mathcal{LR}^3}$ appears at the border collision bifurcation $\xi^{3,r}_{\mathcal{LR}^3}$ being already homoclinic, then it becomes nonhomoclinic at the merging bifurcation $\gamma^3_{\mathcal{LR}^3}$, homoclinic again at the merging bifurcation $\gamma^2_{\mathcal{LR}^3}$ and nonhomoclinic again at the merging bifurcation $\gamma^1_{\mathcal{LR}^3}$. As the map is discontinuous, the boundaries of the attractors are given by two sequences of images of critical points, namely $c^\ell_i = f^i(c^\ell)$ and $c^r_i = f^i(c^r)$, $i \geq 1$, where $c^\ell = f_{\mathcal{L}}(0)$ and $c^r = f_{\mathcal{R}}(0)$. Accordingly, the simplest equations to be solved for the calculation of three merging bifurcations involving the repelling cycle $\mathcal{O}_{\mathcal{LR}^3}$, namely, $\gamma^1_{\mathcal{LR}^3}$, $\gamma^2_{\mathcal{LR}^3}$ and $\gamma^3_{\mathcal{LR}^3}$, are $x_2^{\mathcal{LR}^3} = c^\ell$, $x_2^{\mathcal{LR}^3} = c^r_8$, and $x_2^{\mathcal{LR}^3} = c^\ell_2$, respectively. Similarly the other merging bifurcations shown in Fig. 2 can be determined. Two of them involve the repelling cycle $\mathcal{O}_{\mathcal{LR}^2}$ and three of them, the cycle $\mathcal{O}_{\mathcal{LR}}$.

It is worth to note a difference between continuous and discontinuous cases: In the first example, all six bands are pairwise merging leading to a three-band chaotic attractor. In discontinuous maps not necessarily all the bands are pairwise merging. For example, it can easily be seen in Fig. 2 that at the merging bifurcation $\gamma^1_{\mathcal{LR}^3}$ for decreasing $\mu_{\mathcal{L}}$ all eight bands $\mathcal{B}_0, \ldots, \mathcal{B}_7$ are merging pairwise. By contrast, at the merging bifurcation $\gamma_{\mathcal{LR}^2}$ for increasing $\mu_{\mathcal{L}}$ the bands $\mathcal{B}_1, \ldots, \mathcal{B}_6$ are merging pairwise while the bands $\mathcal{B}_0$, $\mathcal{B}_7$ persist. Indeed, $\gamma_{\mathcal{LR}^2}$ is related to a homoclinic bifurcation of a 3-cycle and hence only six bands are pairwise merging at this bifurcation.

3. Expansion Bifurcation

Consider a 1D piecewise smooth map f depending smoothly on a parameter ν. Assume the existence of a value $\nu = \nu_0$ such that for ν in a one-side neighborhood of ν_0 the map f has a chaotic attractor $\mathcal{A}_k$ consisting of $k \geq 1$ bands, and there is a repelling n-cycle $\mathcal{O}_n$, $n \geq 1$, with a positive *eigenvalue, whose points are located at the boundary of the immediate basin of the attractor. The* expansion bifurcation[5] *occurs if at $\nu = \nu_0$ the attractor $\mathcal{A}_k$ collides with the cycle $\mathcal{O}_n$ and abruptly increases in size.*

As in the case of a merging bifurcation, an expansion bifurcation leads to the appearance of a homoclinic orbit to $\mathcal{O}_n$ which is critical at the bifurcation value. Differently from the case of the merging bifurcation, there are two possibilities for the homoclinic bifurcation of $\mathcal{O}_n$: Before the bifurcation the cycle $\mathcal{O}_n$ can be either one-side homoclinic or not homoclinic. After the bifurcation it becomes double-side homoclinic.

The number of bands of the attractor after an expansion bifurcation depends on the particular system. Below examples are shown in which an expansion bifurcation is related to a homoclinic bifurcation of an n-cycle, and the number of bands is decreased by n (Examples 3.2 and 3.3), or decreased by some number smaller than n (Example 3.1), or remains unchanged (Example 3.4).

Example 3.1. Figure 3 illustrates an expansion bifurcation in the skew tent map (2). For decreasing $a_{\mathcal{R}}$ at the bifurcation $\eta_{\mathcal{RLR}}$ a three-band chaotic attractor collides with the repelling cycle $\mathcal{O}_{\mathcal{RLR}}$ which is one-side homoclinic before the bifurcation. The eigenvalue $\lambda = a_{\mathcal{L}} a^2_{\mathcal{R}}$ of the cycle is positive. After the bifurcation the cycle is double-side homoclinic and the attractor consists of one band only.

As one can easily see in Fig. 3, to calculate the parameter values related to the expansion bifurcation $\eta_{\mathcal{RLR}}$ one can solve any of the following

[5]There are several terms frequently used for this bifurcation, such as *interior crisis* [Grebogi *et al.*, 1982, 1983; Ott, 1993] or *contact bifurcation* [Mira *et al.*, 1996a; Fournier-Prunaret *et al.*, 1997].

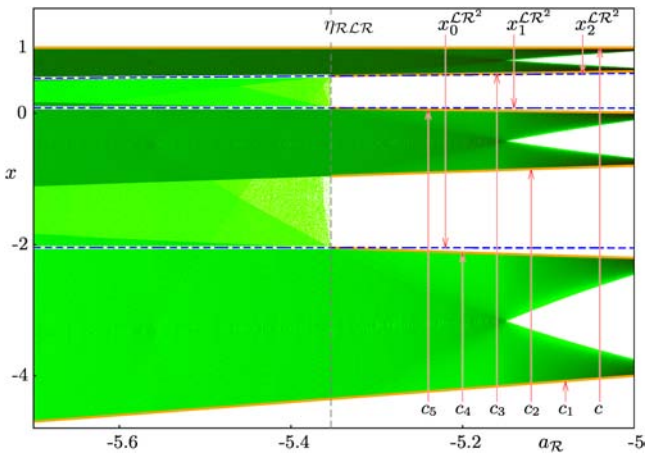

Fig. 3. Expansion bifurcation related to a homoclinic bifurcation of the 3-cycle $\mathcal{O}_{\mathcal{LR}^2}$ in the skew tent map (2). Parameters: $\mu = 1$, $a_{\mathcal{L}} = 0.45$.

equations: $x_0^{\mathcal{RLR}} = c_5$, $x_1^{\mathcal{RLR}} = c_4$, $x_2^{\mathcal{RLR}} = c_3$. Clearly, the last equation contains the image of the critical point of the lowest rank and is therefore most easy to solve.

Example 3.2. Figure 4 shows two expansion bifurcations in the discontinuous map (1). As in the previous example, we observe transitions between three- and one-band attractors, but now they are related to homoclinic bifurcations of the 2-cycle $\mathcal{O}_{\mathcal{LR}}$. This cycle is not homoclinic for the parameter values related to the three-band attractor and it is double-side homoclinic after the expansion bifurcation. To calculate the parameter values related to both expansion bifurcations one has to take into account that the boundaries of the attractors are given now by the images of two critical points, namely $c^{\ell} = f_{\mathcal{L}}(0)$ and $c^{r} = f_{\mathcal{R}}(0)$. As one can easily see in Fig. 4, the parameter values related to one expansion bifurcation can be found by solving any of the equations $x_0^{\mathcal{LR}} = c_1^r$, $x_1^{\mathcal{LR}} = c_2^r$ and the parameter values related to the other bifurcation by solving any of the equations $x_0^{\mathcal{LR}} = c_1^{\ell}$, $x_1^{\mathcal{LR}} = c_2^{\ell}$.

Example 3.3. An expansion bifurcation leads not necessarily to the appearance of a one-band attractor. This occurs if before the expansion bifurcation there are gaps between the bands of the attractor which do not contain points of the cycle undergoing the homoclinic bifurcation. Clearly, these gaps persist after the bifurcation. For example, Fig. 5 shows expansion bifurcations $\eta^{\ell}_{\mathcal{LR}^4}$ and $\eta^{r}_{\mathcal{LR}^4}$ leading from a seven-band attractor to a two-band attractor. The bifurcations are related to homoclinic bifurcations of the 5-cycle $\mathcal{O}_{\mathcal{LR}^5}$ which is nonhomoclinic before the bifurcations and double-side homoclinic after. Before the bifurcations the attractor has six gaps. Five of them disappear after the homoclinic bifurcations of $\mathcal{O}_{\mathcal{LR}^5}$, while one gap, containing the repelling fixed point $\mathcal{O}_{\mathcal{R}}$, persists.

Similarly, the expansion bifurcations $\eta^{\ell}_{\mathcal{LR}^2\mathcal{LR}^6}$ and $\eta^{r}_{\mathcal{LR}^2\mathcal{LR}^6}$ marked in Fig. 5 cause transitions from a 17- to a seven-band attractor. The bifurcations are related to homoclinic bifurcations of the 10-cycle $\mathcal{O}_{\mathcal{LR}^2\mathcal{LR}^6}$. Accordingly, the gaps between the bands of the attractor containing the points of this cycle disappear after the bifurcations, while the gaps containing the points of the 5-cycle $\mathcal{O}_{\mathcal{LR}^4}$ and the fixed point $\mathcal{O}_{\mathcal{R}}$ persist.

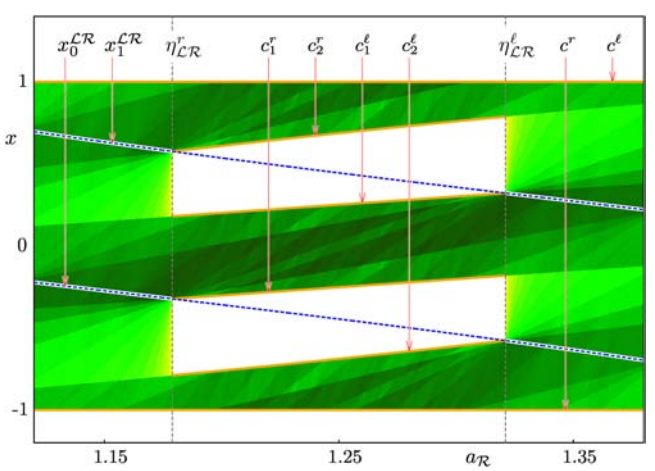

Fig. 4. Expansion bifurcations $\eta^{\ell/r}_{\mathcal{LR}}$ related to homoclinic bifurcations of the 2-cycle $\mathcal{O}_{\mathcal{LR}}$ in map (1). Parameters: $\mu_{\mathcal{L}} = 1$, $\mu_{\mathcal{R}} = -1$, $a_{\mathcal{L}} = 2.5 - a_{\mathcal{R}}$.

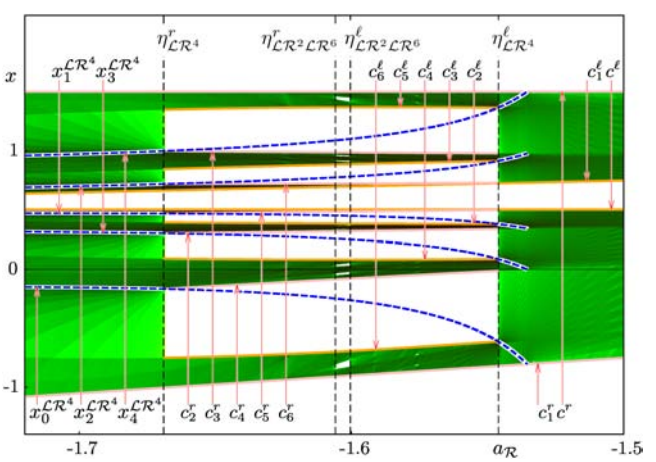

Fig. 5. Expansion bifurcations $\eta^{\ell/r}_{\mathcal{LR}^4}$ related to homoclinic bifurcations of the 5-cycle $\mathcal{O}_{\mathcal{LR}^4}$ in map (1). Parameters: $\mu_{\mathcal{L}} = 0.502$, $\mu_{\mathcal{R}} = 1.502$, $a_{\mathcal{L}} = 0.2$.

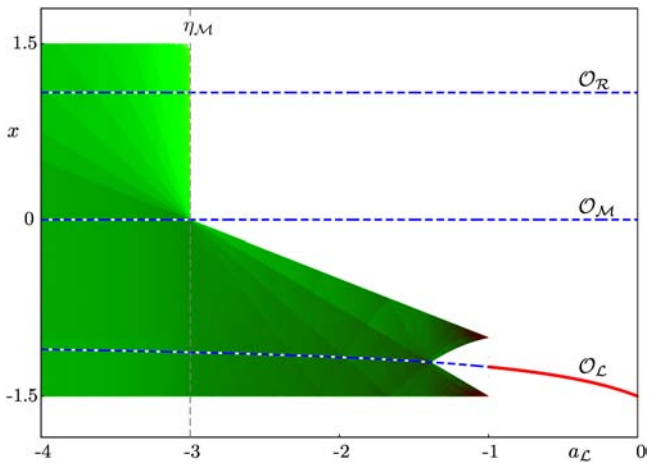

Fig. 6. Expansion bifurcation $\eta_{\mathcal{M}}$ related to a homoclinic bifurcation of the fixed point $\mathcal{O}_{\mathcal{M}}$ in map (3). Parameters: $a_{\mathcal{M}} = 1.5$, $a_{\mathcal{R}} = -5$, $a_{\mathcal{L}} = -2.1$; $a_{\mathcal{L}} = -3.3$.

Example 3.4. The number of bands of the attractor is not necessarily changed at an expansion bifurcation. An example for such a transition in the piecewise linear bimodal map

$$x_{n+1} = \begin{cases} a_{\mathcal{L}} x + (a_{\mathcal{L}} - a_{\mathcal{M}}) & \text{if } x_n < -1 \\ a_{\mathcal{M}} x & \text{if } -1 \le x_n \le 1 \\ a_{\mathcal{R}} x + (a_{\mathcal{M}} - a_{\mathcal{R}}) & \text{if } x_n > 1 \end{cases} \quad (3)$$

is illustrated in Fig. 6, showing a transition from a one-band attractor before the bifurcation to a wider one-band attractor after. The transition is related to a homoclinic bifurcation of the fixed point $\mathcal{O}_{\mathcal{M}} = 0$ which is one-side homoclinic before the bifurcation and double-side homoclinic after.

4. Final Bifurcation

Consider a 1D piecewise smooth map f depending smoothly on a parameter ν. Assume the existence of a value $\nu = \nu_0$ such that for ν in a one-side neighborhood of ν_0 the map f has a chaotic attractor $\mathcal{A}_k$ consisting of $k \ge 2$ bands, and there is a repelling n-cycle $\mathcal{O}_n$, $n \ge 1$, with a positive eigenvalue, whose points are located at the boundary of the immediate basin of the attractor. We say that a final bifurcation[6] *occurs if at $\nu = \nu_0$ the attractor $\mathcal{A}_k$ collides with a point of $\mathcal{O}_n$ and becomes a chaotic repeller.*

Similar to merging and expansion bifurcations, at the bifurcation value the cycle $\mathcal{O}_n$ undergoes a homoclinic bifurcation. The cycle $\mathcal{O}_n$ can be either not homoclinic before the bifurcation and one-side homoclinic after, or one-side homoclinic before the bifurcation and double-side homoclinic after.

If $\mathcal{O}_n$ belongs to the basin boundary separating an attractor from diverging orbits, then after the final bifurcation a generic orbit diverges. Otherwise, after the final bifurcation a generic orbit converges to a different attractor. For piecewise monotone maps with one border point, and in particular, for map (1) the latter case is not possible, thus the final bifurcations can only lead to divergence of the generic orbit.

Example 4.1. As a first example let us consider the final bifurcation $\chi_{\mathcal{L}}$ occurring in the skew tent map (2), as illustrated in Fig. 7. Indeed, at the parameter values corresponding to the condition $\mathcal{O}_{\mathcal{L}} = f_{\mathcal{R}}(c)$, where $c = f(0) = \mu$, the fixed point $\mathcal{O}_{\mathcal{L}}$ undergoes a homoclinic bifurcation and, being nonhomoclinic before the bifurcation, becomes one-side homoclinic after (for $a_{\mathcal{R}} < -1.5$ in Fig. 7). To describe the chaotic repeller existing after the final bifurcation let us first consider the so-called *escape interval*

$$J = (f_{\mathcal{L}}^{-1} \circ f_{\mathcal{R}}^{-1}(\mathcal{O}_{\mathcal{L}}), f_{\mathcal{R}}^{-1} \circ f_{\mathcal{R}}^{-1}(\mathcal{O}_{\mathcal{L}})) \quad (4)$$

defined by the values of $x \in I = (\mathcal{O}_{\mathcal{L}}, f_{\mathcal{R}}^{-1}(\mathcal{O}_{\mathcal{L}}))$ with $f^2(x) < \mathcal{O}_{\mathcal{L}}$. A typical orbit with an initial condition $x_0 \in I$ reaches J in a finite number of iterations and eventually diverges. Figure 7 shows the interval J and a sequence of its preimages.

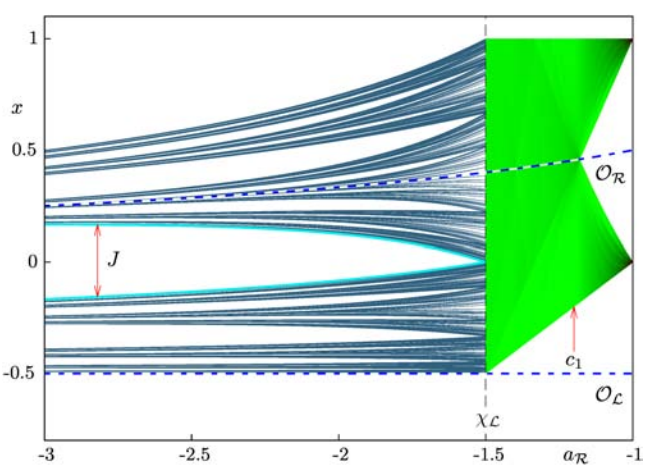

Fig. 7. Final bifurcation $\chi_{\mathcal{L}}$ in the skew tent map (2) related to a homoclinic bifurcation of the fixed point $\mathcal{O}_{\mathcal{L}}$. The escape interval J is marked. Parameters: $a_{\mathcal{L}} = 3$, $\mu = 1$.

[6]This bifurcation is frequently called a *boundary crises* [Grebogi *et al.*, 1982, 1983; Ott, 1993], or an *exterior crisis* [Richetti *et al.*, 1987; Kleczka *et al.*, 1992].

The set[7]

$$\Lambda = I \setminus \bigcup_{k=0}^{\infty} f^{-k}(J) \tag{5}$$

is an invariant Cantor set and constitutes a chaotic repeller. It includes infinitely many repelling cycles and their preimages, as well as uncountably many aperiodic orbits. Note that this chaotic repeller persists after the bifurcation, as no further bifurcations may occur in this parameter range.

Example 4.2. If the map (1) is discontinuous and the slopes $a_{\mathcal{L}}$, $a_{\mathcal{R}}$ are positive, the final bifurcations $\chi_{\mathcal{L}}$ and $\chi_{\mathcal{R}}$ occur at the parameter values defined by the conditions $\mathcal{O}_{\mathcal{L}} = f_{\mathcal{R}}(0)$ and $\mathcal{O}_{\mathcal{R}} = f_{\mathcal{L}}(0)$, respectively (see Fig. 8). For example, at the moment of the homoclinic bifurcation $\chi_{\mathcal{R}}$ of the fixed point $\mathcal{O}_{\mathcal{R}}$, there exists a critical homoclinic orbit to the fixed point including the limiting value $f_{\mathcal{L}}(0)$, and, being nonhomoclinic before the bifurcation, the fixed point is homoclinic after. Let us consider now the situation immediately after the bifurcation $\chi_{\mathcal{R}}$. In this case, a part of the former absorbing interval $[f_{\mathcal{R}}(0), f_{\mathcal{L}}(0)]$ is "cut off" by the repelling fixed point $\mathcal{O}_{\mathcal{R}}$. The remaining part $I = [f_{\mathcal{R}}(0), \mathcal{O}_{\mathcal{R}}]$ contains a chaotic repeller Λ. Similar to Example 4.1, Λ is a Cantor set, as defined by Eq. (5) where the escape interval

$$J = (f_{\mathcal{L}}^{-1}(\mathcal{O}_{\mathcal{R}}), 0) \tag{6}$$

is given by the values of x with $f_{\mathcal{L}}(x) > \mathcal{O}_{\mathcal{R}}$. However, there are also some differences from Example 4.1. Recall that in the skew tent map the chaotic repeller persists for all parameter values after the final bifurcation. By contrast, in the case shown in Fig. 8, repelling cycles belonging to the chaotic repeller which exists after the final bifurcation $\chi_{\mathcal{R}}$, disappear one after another for increasing μ due to border collision bifurcations. Moreover, at the point $\hat{\chi}_{\mathcal{R}}$ the chaotic repeller disappears as well. This parameter value is defined by the condition $\mathcal{O}_{\mathcal{R}} = f_{\mathcal{L}} \circ f_{\mathcal{R}}(0)$ and corresponds to one more homoclinic bifurcation of the fixed point $\mathcal{O}_{\mathcal{R}}$, at which the critical homoclinic orbit includes the limiting value $f_{\mathcal{R}}(0)$. At the bifurcation $\hat{\chi}_{\mathcal{R}}$ this orbit represents the only (except for the fixed points) nondivergent orbit. After the bifurcation $\mathcal{O}_{\mathcal{R}}$ is no longer homoclinic and all orbits (except for the fixed points and preimages of $\mathcal{O}_{\mathcal{R}}$) diverge.

Note that the disappearance of the chaotic repeller can easily be explained by the behavior of the preimages of J. For $\chi_{\mathcal{R}} < \mu < \hat{\chi}_{\mathcal{R}}$ the union of all preimages of J cover the interval I apart from a Cantor set Λ. At the bifurcation $\hat{\chi}_{\mathcal{R}}$ this union covers I except for a countable set (which represents the critical homoclinic orbit existing at this parameter value), and for $\mu > \hat{\chi}_{\mathcal{R}}$ it covers the complete interval I.

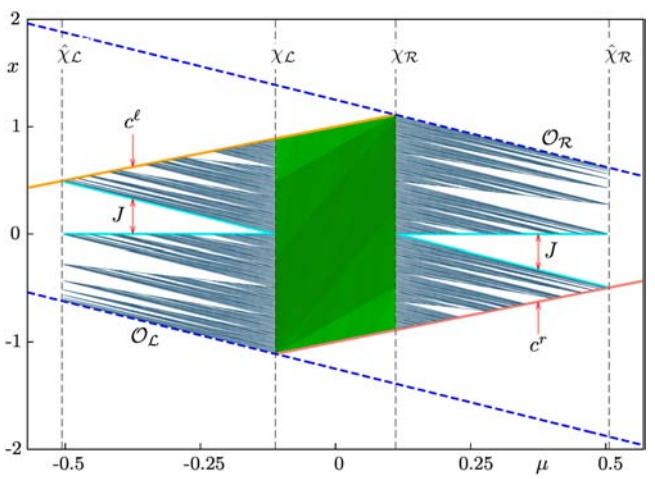

Fig. 8. Final bifurcations $\chi_{\mathcal{L}}$, $\chi_{\mathcal{R}}$ in map (1) related to homoclinic bifurcations of the fixed point $\mathcal{O}_{\mathcal{L}}$ and $\mathcal{O}_{\mathcal{R}}$. The escape intervals J are marked. Parameters: $a_{\mathcal{L}} = a_{\mathcal{R}} = 1.8$, $\mu_{\mathcal{L}} = \mu + 1$, $\mu_{\mathcal{R}} = \mu - 1$.

Example 4.3. In the examples discussed above we considered final bifurcations related to homoclinic bifurcations of fixed points. Indeed, for one-dimensional piecewise monotone maps besides fixed points also a 2-cycle can be involved into a final bifurcation. An example is shown in Fig. 9. Here the 2-cycle $\mathcal{O}_{\mathcal{LR}}$ of map (1) is not homoclinic for $\mu_{\mathcal{R}} \in (\chi^{\ell}_{\mathcal{LR}}, \chi^{r}_{\mathcal{LR}})$. In this parameter range $\mathcal{O}_{\mathcal{LR}}$ separates the basin of the chaotic attractor from the region of divergent behavior.

The conditions of the final bifurcations $\chi^{\ell}_{\mathcal{LR}}$ and $\chi^{r}_{\mathcal{LR}}$ related to homoclinic bifurcations of $\mathcal{O}_{\mathcal{LR}}$ are given by $x_0^{\mathcal{LR}} = f_{\mathcal{L}}(0)$ and $x_1^{\mathcal{LR}} = f_{\mathcal{R}}(0)$, respectively. The chaotic repeller remaining after these bifurcations is a Cantor set as given by Eq. (5), whereby the interval $I = [x_0^{\mathcal{LR}}, x_1^{\mathcal{LR}}]$ is the same for

[7]Recall that the inverse function f^{-1} for the skew tent map has two values, so that the set $f^{-k}(J)$, $k \geq 1$, consists of 2^k disjoint intervals.

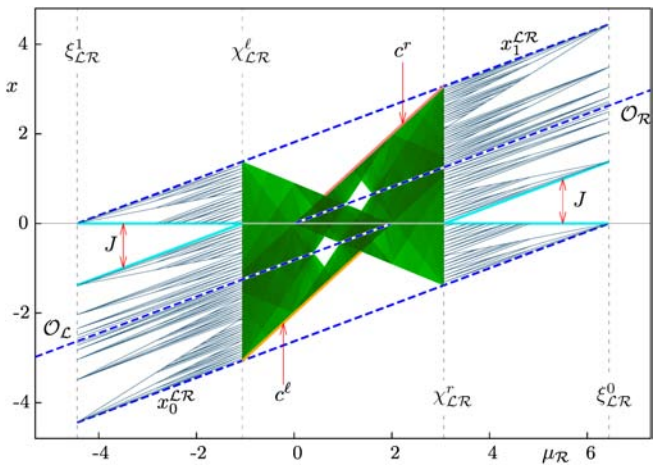

Fig. 9. Final bifurcations $\chi^{\ell}_{\mathcal{LR}}$ and $\chi^{r}_{\mathcal{LR}}$ in map (1) related to homoclinic bifurcations of the 2-cycle $\mathcal{O}_{\mathcal{LR}}$. The escape intervals J are marked. Parameters: $a_{\mathcal{L}} = a_{\mathcal{R}} = -1.45$, $\mu_{\mathcal{L}} = \mu_{\mathcal{R}} - 2$.

both bifurcations $\chi^{\ell}_{\mathcal{LR}}$ and $\chi^{r}_{\mathcal{LR}}$, while the escape intervals are different. After the final bifurcation $\chi^{r}_{\mathcal{LR}}$ the escape interval is

$$J = (0, f_{\mathcal{R}}^{-1}(x_1^{\mathcal{LR}})) \tag{7}$$

and after $\chi^{\ell}_{\mathcal{LR}}$ it is

$$J = (f_{\mathcal{L}}^{-1}(x_0^{\mathcal{LR}}), 0). \tag{8}$$

As one can see in Fig. 9, in both cases the chaotic repellers persist only up to the points $\xi^0_{\mathcal{LR}}$ and $\xi^1_{\mathcal{LR}}$ at which the cycle $\mathcal{O}_{\mathcal{LR}}$ undergoes a border collision bifurcation and disappears.

5. Bifurcations of Chaotic Attractors Related to a Fold Border Collision Bifurcation

All three kinds of bifurcations discussed above (the merging, the expansion, and the final bifurcation) occur both in continuous and in discontinuous maps. Additionally, there exists a transformation of chaotic attractors which occurs in piecewise smooth *continuous* maps only. Recall that in a continuous map cycles may appear via a fold border collision bifurcation. This bifurcation leads to the appearance of a pair of complementary cycles, from which one is necessarily repelling, and the other one may be attracting or repelling. If both cycles are repelling, this may lead to the following bifurcation of chaotic attractors.

Let us assume that

(1) *before the bifurcation the map f has a one-band*[8] *chaotic attractor given by an interval J;*
(2) *a fold border collision bifurcation*[9] *leads to the appearance of a pair of repelling n-cycles $\mathcal{O}_n$ and $\mathcal{O}'_n$ belonging to J, $n \geq 1$, with the eigenvalues satisfying*

$$\lambda(\mathcal{O}_n) < -1, \quad \lambda(\mathcal{O}'_n) > 1; \tag{9}$$

(3) *after the bifurcation the map f^n has n local absorbing intervals inside J,*

then the effect of the fold border collision bifurcation is the following:

- *if the cycle $\mathcal{O}_n$ appears double-side homoclinic, then after the bifurcation an n-band chaotic attractor $\mathcal{A}_n$ appears*;
- *if the cycle $\mathcal{O}_n$ appears nonhomoclinic, then after the bifurcation a $2^k n$-band chaotic attractor $\mathcal{A}_{2^k n}$ appears, $k \geq 1$.*

In both cases, the repelling cycle $\mathcal{O}'_n$ belongs to the boundary of the immediate basin of the chaotic attractor existing after the bifurcation ($\mathcal{A}_n$ or $\mathcal{A}_{2^k n}$). Therefore, as the parameters approach the bifurcation value, the attractor ($\mathcal{A}_n$ or $\mathcal{A}_{2^k n}$) shrinks to the cycle $\mathcal{O}_n \equiv \mathcal{O}'_n$ containing the border point. The total basin boundary of the attractor includes a chaotic repeller, so that the cycle $\mathcal{O}'_n$ is necessarily one-side homoclinic after the bifurcation.

This statement can be proved using the skew tent map as a normal form for border collision bifurcations.[10]

Example 5.1. To illustrate the effect of a fold border collision bifurcation leading to a bifurcation of chaotic attractors described above in the most simple case related to the appearance of two repelling

[8]If f has an m-band chaotic attractor, we consider the iterated map f^m. This is always possible, as f is continuous and hence its multiband chaotic attractors are cyclic.
[9]Also referred to as a nonsmooth fold bifurcation [di Bernardo *et al.*, 2008].
[10]For an example of the use of the skew tent map as a normal form for border collision bifurcations, we refer to [Sushko & Gardini, 2010].

fixed points, let us consider the following map:

$$x_{n+1} = \begin{cases} f_{\mathcal{LL}}(x_n) = a_{\mathcal{LL}}(x_n + 1) - a_{\mathcal{L}} + \mu \\ \qquad\qquad\qquad\qquad \text{if } x_n < -1 \\ f_{\mathcal{L}}(x_n) = a_{\mathcal{L}} x_n + \mu \quad \text{if } -1 \le x_n < 0 \\ f_{\mathcal{R}}(x_n) = a_{\mathcal{R}} x_n + \mu \quad \text{if } 0 \le x_n < 1 \\ f_{\mathcal{RR}}(x_n) = a_{\mathcal{RR}}(x_n - 1) + a_{\mathcal{R}} + \mu \\ \qquad\qquad\qquad\qquad \text{if } 1 \le x_n \end{cases} \tag{10}$$

with $a_{\mathcal{LL}} < 0$, $a_{\mathcal{L}} > 0$, $a_{\mathcal{R}} < 0$, $a_{\mathcal{RR}} > 0$. The fixed points of map (10) related to its middle branches, namely $\mathcal{O}_{\mathcal{L}} = \frac{\mu}{1-a_{\mathcal{L}}}$ and $\mathcal{O}_{\mathcal{R}} = \frac{\mu}{1-a_{\mathcal{R}}}$, do not exist if $\mu < 0$ and appear at $\mu = 0$ via a fold border collision bifurcation.

A transition (for μ increasing through zero) from a broad one-band attractor to a narrow one-band attractor $\mathcal{A}_1$ which appears due to the border collision bifurcation of the fixed points $\mathcal{O}_{\mathcal{L}}$, $\mathcal{O}_{\mathcal{R}}$ is shown in Fig. 10(a). At the used parameter values the interval J before the bifurcation (for $\mu < 0$) is given by

$$J = [f_{\mathcal{R}}(1), f_{\mathcal{LL}} \circ f_{\mathcal{R}}(1)]. \tag{11}$$

Clearly, it contains the border point $x = 0$ at which the fixed points $\mathcal{O}_{\mathcal{L}}$ and $\mathcal{O}_{\mathcal{R}}$ appear at $\mu = 0$. As $a_{\mathcal{L}} > 1$, $a_{\mathcal{R}} < -1$, both of them are repelling and in terms of the description of the bifurcation given above we have $\mathcal{O}_{\mathcal{L}} = \mathcal{O}'_n$, $\mathcal{O}_{\mathcal{R}} = \mathcal{O}_n$. The absorbing interval appearing after the bifurcation has an immediate basin bounded by $\mathcal{O}_{\mathcal{L}}$ and its rank-one preimage by $f_{\mathcal{R}}^{-1}$. Inside this interval there is a narrow one-band chaotic attractor $\mathcal{A}_1$. As the boundaries of $\mathcal{A}_1$ are given by μ and $f_{\mathcal{R}}(\mu)$, for μ decreasing to zero the attractor collapses to a fixed point at the border. After the bifurcation, for $\mu > 0$, the fixed point $\mathcal{O}_{\mathcal{R}}$ is double-side homoclinic (because $f_{\mathcal{L}}^{-1}(\mathcal{O}_{\mathcal{R}}) > f_{\mathcal{R}}(\mu)$), and the fixed point $\mathcal{O}_{\mathcal{L}}$ is one-side homoclinic.

Transitions from a one-band to a 2^k-band chaotic attractors for map (10) are illustrated in Figs. 10(b) and 10(c) for $k = 1, 2$. In both cases the fixed point $\mathcal{O}_{\mathcal{R}}$ appears nonhomoclinic (as $f_{\mathcal{L}}^{-1}(\mathcal{O}_R) < f_{\mathcal{R}}(\mu)$). To explain the difference between the cases shown in Figs. 10(b) and 10(c) one has to note that at the fold border collision bifurcation at which the fixed points $\mathcal{O}_{\mathcal{L}}$, $\mathcal{O}_{\mathcal{R}}$ appear, also an infinite family of repelling 2^j-cycles, $j = 1, 2, 3, \ldots$, appear, namely the so-called harmonics of $\mathcal{O}_{\mathcal{R}}$. If $\mathcal{O}_{\mathcal{R}}$ appears homoclinic [as in Fig. 10(a)] then all the harmonics appear homoclinic as well. If $\mathcal{O}_{\mathcal{R}}$ appears nonhomoclinic, then some of the harmonics may appear nonhomoclinic also. In this case, let k be the smallest index, for which the harmonic 2^k-cycle appears homoclinic, then we observe a transition to a 2^k-band chaotic attractor. For example, in the case shown in Fig. 10(b) all harmonic cycles are homoclinic (i.e. $k = 1$), so that we observe a transition to a two-band chaotic attractor. By contrast, in the case shown in Fig. 10(c) the 2-cycle $\mathcal{O}_{\mathcal{LR}}$ is nonhomoclinic and the first harmonic cycle which is homoclinic is for $k = 2$, that means a 4-cycle. Accordingly, this bifurcation leads to the appearance of a four-band chaotic attractor.

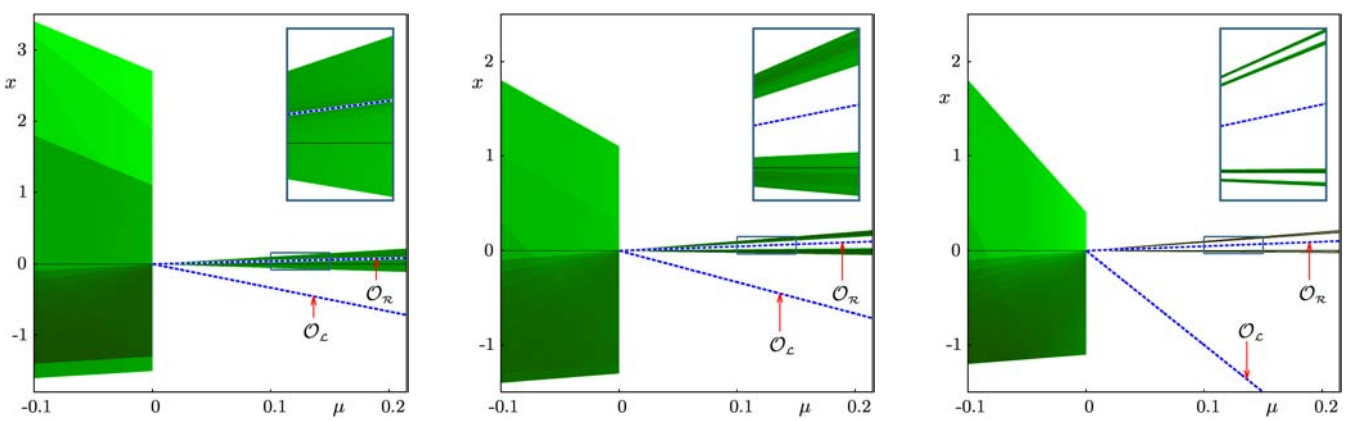

Fig. 10. Transition from a one-band to a (a) one-band, (b) two-band and (c) four-band chaotic attractor in map (10), related to the fold border collision bifurcation at which the fixed points $\mathcal{O}_{\mathcal{L}}$, $\mathcal{O}_{\mathcal{R}}$ appear. Insets show the marked rectangles enlarged. Parameters: $a_{\mathcal{RR}} = 2$ and (a) $a_{\mathcal{LL}} = -8$, $a_{\mathcal{L}} = 1.3$, $a_{\mathcal{R}} = -1.5$; (b) $a_{\mathcal{LL}} = -8$, $a_{\mathcal{L}} = 1.3$, $a_{\mathcal{R}} = -1.2$; (c) $a_{\mathcal{LL}} = -15$, $a_{\mathcal{L}} = 1.1$, $a_{\mathcal{R}} = -1.1$.

In the skew tent map (2) the discussed type of bifurcations of chaotic attractors can be related to a fold border collision bifurcation of basic cycles[11] with periods $n \geq 3$ only, and the harmonic cycles are always homoclinic. Accordingly, the fold border collision bifurcation of a basic n-cycle in the skew tent map leads either to the appearance of an n-band or a $2n$-band chaotic attractor.

Acknowledgments

The work of the first author was supported by the European Community within the scope of the project "Multiple-discontinuity induced bifurcations in theory and applications" (Marie Curie Action of the 7th Framework Programme, Contract Agreement N. PIEF-GA-2011-300281).

References

Alligood, K., Sander, E. & Yorke, J. [2002] "Explosions: Global bifurcations at heteroclinic tangencies," *Erg. Th. Dyn. Syst.* **22**, 953–972.

Avrutin, V. & Schanz, M. [2008] "On the fully developed bandcount adding scenario," *Nonlinearity* **21**, 1077–1103.

Avrutin, V. & Sushko, I. [2012] "A gallery of bifurcation scenarios in piecewise smooth 1D maps," *Global Analysis of Dynamic Models in Economics, Finance and the Social Sciences*, eds. Bischi, G.-I., Chiarella, C. & Sushko, I. (Springer), pp. 369–395.

Avrutin, V., Sushko, I. & Gardini, L. [2014] "Cyclicity of chaotic attractors in one-dimensional discontinuous maps," *Math. Comput. Simul.* (*Special Issue "Discontinuous Dynamical Systems*: *Theory and Numerical Methods"*) **95**, 126–136.

Banerjee, S., Yorke, J. A. & Grebogi, C. [1998] "Robust chaos," *Phys. Rev. Lett.* **80**, 3049–3052.

Crutchfield, J. & Young, K. [1990] "Computation at the onset of chaos," *Entropy, Complexity, and the Physics of Information*, ed. Zurek, W. H. (Addison-Wesley), pp. 223–269.

di Bernardo, M., Budd, C. J., Champneys, A. R. & Kowalczyk, P. [2008] *Piecewise-Smooth Dynamical Systems*: *Theory and Applications*, Applied Mathematical Sciences, Vol. 163 (Springer).

Fournier-Prunaret, D., Mira, C. & Gardini, L. [1997] "Some contact bifurcations in two-dimensional examples," *Grazer Mathematishe Berichte* **334**, 77–96.

Gardini, L. [1994] "Homoclinic bifurcations in n-dimensional endomorphisms, due to expanding periodic points," *Nonlin. Anal.*: *Th. Meth. Appl.* **23**, 1039–1089.

Gardini, L., Cathala, J. C. & Mira, C. [1996] "Contact bifurcations of absorbing and chaotic areas in two-dimensional endomorphisms," *Iteration Theory*, ed. Forg-Rob, W. (World Scientific, Singapore), pp. 100–111.

Gardini, L., Sushko, I., Avrutin, V. & Schanz, M. [2011] "Critical homoclinic orbits lead to snap-back repellers," *Chaos Solit. Fract.* **44**, 433–449.

Grebogi, C., Ott, E. & Yorke, J. A. [1982] "Chaotic attractors in crisis," *Phys. Rev. Lett.* **48**, 1507–1510.

Grebogi, C., Ott, E. & Yorke, J. A. [1983] "Crisis: Sudden changes in chaotic attractors and transient chaos," *Physica D* **7**, 181.

Grebogi, C., Ott, E., Romeiras, F. & Yorke, J. [1987] "Critical exponents for crisis-induced intermittency," *Phys. Rev. A* **36**, 5365.

Kaneko, K. [1989] "Spatiotemporal chaos in one- and two-dimensional coupled map lattices," *Physica D* **37**, 60–82.

Kleczka, M., Kreuzer, E. & Schiehlen, W. [1992] "Local and global stability of a piecewise linear oscillator," *Phil. Trans. Roy. Soc. A* **338**, 533–546.

Maistrenko, Y. L., Sushko, I. & Gardini, L. [1998] "About two mechanisms of reunion of chaotic attractors," *Chaos Solit. Fract.* **9**, 1373–1390.

Marotto, F. [1978] "Snap-back repellers imply chaos in R^n," *J. Math. Anal. Appl.* **63**, 199–223.

Marotto, F. [2005] "On redefining a snap-back repeller," *Chaos Solit. Fract.* **25**, 25–28.

Mira, C. & Narayaninsamy, T. [1993] "On behaviors of two-dimensional endomorphisms: Role of the critical curves," *Int. J. Bifurcation and Chaos* **3**, 187–194.

Mira, C., Gardini, L., Barugola, A. & Cathala, J.-C. [1996a] *Chaotic Dynamics in Two-Dimensional Noninvertible Maps*, World Scientific Series on Nonlinear Science, Vol. 20 (World Scientific, NJ).

Mira, C., Rauzy, C., Maistrenko, Y. & Sushko, I. [1996b] "Some properties of a two-dimensional piecewise-linear noninvertible map," *Int. J. Bifurcation and Chaos* **6**, 2299–2319.

Ott, E. [1993] *Chaos in Dynamical Systems* (Cambridge University Press, Cambridge), pp. 26–31.

Richetti, P., De Kepper, P., Roux, J. & Swinney, H. [1987] "A crisis in the Belousov–Zhabotinskii reaction: Experiment and simulation," *J. Statist. Phys.* **48**, 977–990.

Robert, C., Alligood, K., Ott, E. & Yorke, J. [2000] "Explosions of chaotic sets," *Physica D* **144**, 44–61.

Sushko, I. & Gardini, L. [2010] "Degenerate bifurcations and border collisions in piecewise smooth 1D and 2D maps," *Int. J. Bifurcation and Chaos* **20**, 2045–2070.

[11]Cycles associated with symbolic sequences $\mathcal{LR}^m$ or $\mathcal{RL}^m$, also called maximal, principal or atomic cycles.